THE ASTROPHYSICAL JOURNAL, 302:777–784, 1986 March 15

THE MAGNETIC FIELD OF THE BY DRACONIS FLARE STAR EQ VIRGINIS[1]

STEVEN H. SAAR AND JEFFREY L. LINSKY[2]
Joint Institute for Laboratory Astrophysics, University of Colorado and National Bureau of Standards
AND
JACQUES M. BECKERS
Multiple Mirror Telescope Observatory, University of Arizona
Received 1985 June 13; accepted 1985 September 5

ABSTRACT

We apply a new Zeeman analysis procedure, which includes radiative transfer effects and compensation for blends, to high-resolution, high–signal-to-noise line profiles of the BY Draconis–type flare star EQ Vir obtained with the Multiple Mirror Telescope. Using a number of lines with effective Landé g factors ranging from 0.5 to 2.5, and two different analysis methods, we find a mean field of 2500 ± 300 G covering $80\% \pm 15\%$ of EQ Vir. We believe this result is important for several reasons: (1) It is the first positive detection of a magnetic field in a BY Draconis–type flare star, confirming that magnetic fields are certainly present on these stars. Lack of prior detections in polarized light suggests that these active stars have complex magnetic topologies like that of the Sun. (2) EQ Vir exhibits a substantially higher surface-averaged field ($\langle B \rangle \equiv fB$) than any previously measured star. We attribute this difference to the short rotational period and high angular velocity of EQ Vir compared with the other stars, and presume that the larger values of $\langle B \rangle$ are due to enhanced field generation by the dynamo process. (3) The measured value of 2500 G for the photospheric field strength on EQ Vir is similar to the value derived by assuming equipartition of magnetic and thermal energy densities in the photosphere and scaling from the solar network fields. This suggests that equipartition may somehow determine the mean field strength in the nonspotted portion of a flare star photosphere. The value of 2500 G for the field strength is also smaller than predicted theoretically.

Subject headings: stars: flare — stars: late-type — stars: magnetic

I. INTRODUCTION

The hypothesis that magnetic fields are the primary cause of activity in late-type stars is now generally accepted. Strong but indirect evidence for the presence of these fields comes in many forms. The existence in cool stars of stellar chromospheres, coronae, spots, and flares, for example, argues for magnetic activity, since analogous solar phenomena are spatially and theoretically linked to strong, complex fields (e.g., Vaiana and Rosner 1978; Linsky 1980, 1983; Zwaan 1981).

In a fundamental sense, however, the detailed relationships among surface magnetic fields, the interior layers from which they arise, and the chromosphere and corona that they heat remain largely unknown, even for the Sun. Direct measurements of surface magnetic fields are clearly necessary for substantial progress on this problem. Unfortunately, such measurements are hampered by the near cancellation of circular polarization owing to the mix of opposing field polarities on the unresolved stellar disks. Advances in detector technology and analysis techniques (e.g., Robinson 1980), however, make it now possible to measure stellar fields in unpolarized light (Robinson, Worden, and Harvey 1980, hereafter RWH; Marcy 1984; Gray 1984*a*). The new methods have yielded 21 positive detections of field strengths and fractional surface area coverages (filling factors) to date from observations of 33 G and K dwarfs. These successes notwithstanding, a thorough analysis of magnetic activity requires that such measurements be extended to cover the widest possible range in stellar parameters. Some research along these lines has begun with work on active giants (Giampapa, Golub, and Worden 1983; Marcy and Bruning 1984). Despite several attempts, however (e.g., Vogt 1980; Brown and Landstreet 1981), there have been no unambiguous field measurements for one of the most active categories of dwarfs: the flare stars. (In particular, the proposed detection of a 40 kG field on BY Dra by Anderson, Hartmann, and Bopp 1976 is now believed to be spurious [Anderson 1979].)

Flare stars exhibit sporadic luminosity increases that, like solar flares, are characterized by enhanced emission-line and continuum strengths and small sizes (Cram and Woods 1982). The total flare energy, in contrast, frequently is 100 times that of the largest solar flare. On this basis Bopp (1974), Kunkel (1975), and others have suggested that the intense stellar flares originate in regions of extremely strong magnetic activity. Mullan (1974) has developed models supporting this concept that require field strengths as high as 20 kG on dMe flare stars. The nonflaring state of these stars also seems to be qualitatively different from that of the Sun (e.g., Linsky *et al.* 1982; Cram and Mullan 1979). Their quiescent X-ray emission is often orders of magnitude larger than the Sun's, and many dKe and dMe stars also exhibit the so-called BY Draconis syndrome (Kunkel 1975): low-amplitude photometric variability attributable to large cool "starspots." Flare stars thus offer a valuable laboratory in which magnetically related activity can be studied at levels far in excess of that seen on normal stars. Measurements of magnetic fields for these stars are therefore of great interest. This paper describes the first such measurement

[1] Observations reported here were made at the Multiple Mirror Telescope Observatory, a joint facility of the University of Arizona and the Smithsonian Institution.

[2] Staff Member, Quantum Physics Division, National Bureau of Standards.

for a flare star: the BY Draconis variable EQ Vir (=Gl 517 = HD 118100).

II. OBSERVATIONS

EQ Vir is a young, single, rapidly rotating flare star with a photometric period of 3.96 days (Bopp and Fekel 1977; Vogt, Soderblom, and Penrod 1983). It possesses strong chromospheric and transition region emission lines (Linsky *et al.* 1982) and a substantial X-ray luminosity (log $L_x = 29.4$; Vaiana *et al.* 1981). It is also relatively bright ($m_V = 9.34$) and of early enough spectral type (dK5e) that molecular-line blending in the optical spectrum is not ruinous. EQ Vir is thus amenable to magnetic field analysis of the type first formulated by Robinson (1980).

Recognition that polarization studies are ineffective on late-type stars led Robinson to develop a technique to measure magnetic fields using unpolarized line profiles. We also adopt this approach, taking advantage of the slight, usually unresolved splitting of an unpolarized line profile into σ and π components due to the Zeeman effect. For a simple triplet, the π component is unshifted, while the σ components are displaced by $\pm\Delta\lambda_B$, given by

$$\Delta\lambda_B = 4.67 \times 10^{-13}\lambda(\text{Å})^2 gB\,, \qquad (1)$$

where g is the effective Landé value, and B is the magnetic field strength in gauss. We measure this broadening by a detailed comparison of magnetically sensitive and insensitive (high- and low-g) line profiles. Lines analyzed were from the area around the Fe I λ6173 ($g = 2.5$) line used by Marcy (1984).

Observations of EQ Vir were made using the Cassegrain echelle spectrograph and intensified dual Reticon system (Latham 1982) on the 4.5 m Multiple Mirror Telescope (MMT). The echelle allowed some 60 Å of the spectrum and sky background to be recorded simultaneously, permitting several low- and high-g lines to be used in the analysis. A 25 μm (= 0".32) slit was employed, which, although it lost a factor of 3–4 in light, allowed us to obtain the highest resolution possible. The internal averaging electronics of the 1024 diode Reticon (which centroids light events to one-quarter of a diode) were bypassed, permitting all 4096 pixels to be recorded. The resulting resolution, as measured by the FWHM of Th-Ar calibration-lamp emission lines, was 0.075 Å (~5 pixels), corresponding to $\lambda/\Delta\lambda = 80{,}000$ (= 3.6 km s^{-1}). Integration times were typically 30 minutes each, and were preceded and followed by a Th-Ar lamp exposure. Inspection of the lamp spectra showed the instrumental profile to be stable over the course of the observations. Flat fields and dark frames were taken at the end of each night. A summary of the EQ Vir observations and adopted stellar parameters is given in Tables 1 and 2.

The initial data reductions proceeded in the following fashion. Each spectrum was dark- and sky-subtracted, and divided by the sum of the flat fields. We modeled a slight distortion of the wavelength scale with a fifth-order polynomial, interpolated the spectra onto a linear wavelength grid, and registered and co-added them. The data were then resampled by summing pairs of adjacent pixels, resulting in ~2.5 pixels per resolution element, and the two nights of data were added as well to improve the signal-to-noise ratio (S/N). Our final reduced spectrum of EQ Vir (S/N ~ 55/1) thus represents the sum of two "snapshots" of the star taken ~$\frac{1}{4}$ orbital period apart, with contributions to the profile from some 75% of the star's surface. The central 42 Å of our final reduced spectrum is shown in Figure 1.

TABLE 1

SUMMARY OF EQ VIRGINIS OBSERVATIONS

Date	Exposure (min)	S/N	Number of Counts per Resolution Element
1983 Jan 6	90	40	3600
1983 Jan 7	105	35	2750
Combined	195	55	6350

TABLE 2

SUMMARY OF ADOPTED EQ VIRGINIS PARAMETERS

Parameter	Value	Source
Spectral type	dK5e	Kunkel 1975
$B-V$	1.18	Kunkel 1975
$T_{\rm eff}$	4250 K	mean of published values
$v \sin i$[a]	10.8 km s^{-1}	Vogt, Soderblom, and Penrod 1983
ζ macro[a]	3.0 km s^{-1}	Vogt, Soderblom, and Penrod 1983
ξ micro[a]	2.0 km s^{-1}	Gray 1976
B[a]	1000 G	initial guess $\approx \Delta\lambda_D$
f[a]	0.3	initial guess

[a] Initial values of parameters at the beginning of the iterative profile fits.

III. DATA ANALYSIS

a) *The Model*

Existing techniques for analyzing stellar magnetic fields have two deficiencies: inadequate treatment of radiative transfer effects and weak line blends. Both shortcomings can appreciably alter the derived magnetic parameters (Gray 1984*a*; Kurucz and Hartmann 1984; Saar 1986), and both become increasingly significant in stars of later spectral types, where line saturation and blanketing by molecular bands become important. To correct these shortcomings, we have developed a simple analysis which includes Zeeman radiative transfer and blending effects and has the flexibility of several modes of application. The procedure is discussed in more detail elsewhere (Saar 1986); we only outline it briefly here.

Essentially, our analysis scheme is a stellar analog of the one developed by Auer, Heasley, and House (1977) for the study of solar Stokes vector profiles. We assume a Milne-Eddington atmosphere, LTE, and a source function linear in τ ($S_\nu = a + b\tau$), and we ignore magneto-optical effects. Under these conditions, the solution to the magnetic transfer equation for the I-component of the Stokes vector becomes

$$I_\nu = a + \frac{1}{2} b\mu\left(\frac{1}{1+\eta_+} + \frac{1}{1+\eta_-}\right), \qquad (2)$$

where $\eta_\pm$ are the line-to-continuum opacity ratio functions for oppositely elliptically polarized light (Stepanov 1958) given by

$$\eta_\pm = \tfrac{1}{2}\eta_p - \tfrac{1}{2}(\eta_r + \eta_b)\sin^2\gamma + \tfrac{1}{2}(\eta_r + \eta_b) \pm \tfrac{1}{2}\{[\eta_p - \tfrac{1}{2}(\eta_r + \eta_b)]^2 \sin^4\gamma + (\eta_r - \eta_b)^2\cos^2\gamma\}^{1/2}. \qquad (3)$$

Here γ is the angle between the line of sight and the magnetic field; for simplicity we adopt a disk-averaged value $\gamma = \langle\gamma\rangle = 34°$ (Marcy 1982). The parameters η_p, η_b, and η_r are the line-to-continuum opacity ratio functions for the π component(s) and the "blue-" and "red-"shifted σ com-

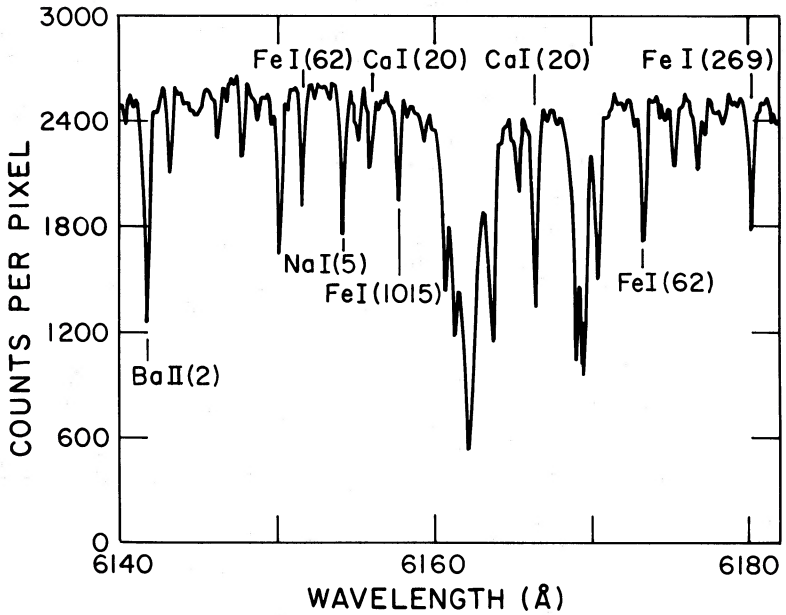

FIG. 1.—Central 42 Å of the reduced EQ Vir spectrum. The data have been smoothed by a Fourier optimum filter. The spectrum is dominated by the strong Ca I λ6162.2 feature near the center.

ponent(s), respectively. They depend on the line opacity η_0, the magnetic field B, and the Doppler width $\Delta\lambda_D = (\lambda_0/c)(2kT_{\rm eff}/m + \xi^2)^{1/2}$, where ξ is the microturbulent velocity. We normalize I_ν to the continuum ($I_c = a + b\mu$), invert the profile, select a specific $I_\nu(\mu)$ to best represent the disk-averaged profile, and convolve this with Gray's rotational and radial-tangential macroturbulent velocity (ζ) broadening functions [$V(\lambda)$, $M(\lambda)$; Gray 1976] and the known instrumental profile [$i(\lambda)$] to derive our model flux profile. The resulting function,

$$F = \left\{\frac{\beta\mu}{1+\beta\mu}\left[1 - \frac{1}{2}\left(\frac{1}{1+\eta_+} + \frac{1}{1+\eta_-}\right)\right]\right\} * V(\lambda) * M(\lambda) * i(\lambda)\,, \quad (4)$$

(where $*$ indicates a convolution and $\beta \equiv b/a$) represents the line profile from a rotating star completely covered with a uniform magnetic field. For a star having uniformly distributed magnetic regions covering some fraction f of its surface, and assuming that the atmospheric properties of the magnetic and nonmagnetic regions are identical, the full expression for the inverted model is

$$F = fF_{\rm mag} + (1-f)F_{\rm nonmag}\,, \quad (5)$$

with

$$F_{\rm nonmag} = \left[\frac{\beta\mu}{1+\beta\mu}\left(1 - \frac{1}{1+\eta}\right)\right] * V(\lambda) * M(\lambda) * i(\lambda)\,. \quad (6)$$

Here η is the opacity function in the nonmagnetic region (a function of η_0 and $\Delta\lambda_D$ alone). Because it is a convolution of simple analytic functions, the model is amenable to a χ^2 hypersurface search for the best parameter values. Once $v \sin i$, ζ, and ξ are determined from modeling low-g lines, a high-g line may be fitted with only three free parameters (η_0, f, and B), permitting rapid, unbiased computer determination of the optimum values of f and B.

There are inherent in the new analysis technique several advantages over those used in the past. First, it accounts for radiative transfer effects in a more complete way. Although efforts toward treating saturation in the individual thermal profiles have recently been made (Marcy and Bruning 1984; Gray 1984*a*), our technique is the first to treat the full problem, including magnetic saturation effects. In the process, it eliminates the "convolution" and "Sears relation" assumptions employed previously to compute Zeeman split profiles, which are accurate only in the weak line ($\eta_0 \ll 1$) limit. A second advantage is the way in which our method deals with scaling. Owing to the desaturation and broadening effects of magnetic splitting, it is difficult to establish the intrinsic shape (i.e., the η_0 and ξ values) of a high-g line *a priori*. We estimate these parameters by modeling a low-g line, and adjust the model's opacity (η_0) until its equivalent width matches that of the high-g line (a somewhat similar approach was taken by Marcy and Bruning 1984). We then use the derived ξ and the adjusted η_0 values as initial estimates for the ξ and η_0 values for the high-g line. This explicit consideration of line saturation effects improves on early methods that simply scaled a low-g line by a constant factor. Our technique also permits greater latitude in the choice of low-g comparison lines, since it can iterate on both η_0 and $\Delta\lambda_D$. Small deviations in the comparison lines from the ideal (owing, for example, to differences in atomic structures or broadening parameters) are thus unimportant, and a larger sample of lines can be used to improve the determinations of f and B statistically (Gray 1984*a*). We can also fit groups of lines simultaneously, using, for example, (η_{0i}, ξ, $v \sin i$) fits to lines of various opacities (η_{0i}) to determine $v \sin i$ to greater accuracy. Finally, we have devised several methods of applying the general model in ways that minimize blends (Saar 1986). We apply two of these methods here to the line profiles of EQ Vir.

b) Applications to EQ Virginis

The initial method of analysis we used was a simple fit of the EQ Vir line profiles to the flux model described in § III*a*. First, however, we addressed the subject of blends in detail. The lines

TABLE 3

LINES USED IN THE ANALYSES

Identification	λ (Å)	Multiplet No.[a]	Lower Level[a] Excitation Potential (eV)	Effective Landé *g*	Analysis Type(s)[b]	$EW_{\odot}$[a] (mÅ)	$EW_{EQ\ Vir}$ (mÅ)
Ba II	6141.727	2	0.70	1.100	V	113	203
Fe I	6151.623	62	2.18	1.833	M	41	93
Na I	6154.230	5	2.10	1.333	V, M	27	116
Ca I	6156.030	20	2.52	2.000	M	7	60
Fe I	6157.733	1015	4.07	1.250	V	48	71
Ca I	6166.44	20	2.52	0.500	V, M	54	148
Fe I	6173.341	62	2.22	2.500	M	50	126
Fe I	6180.209	269	2.73	0.625	V, M	40	98

[a] From Moore, Minnaert, and Houtgast 1966.
[b] V = used in velocity broadening analysis; M = used in magnetic analysis.

chosen for analysis (see Table 3) were selected initially to be as free of blends as possible, but in a star as cool as EQ Vir it is doubtful that *any* line profile is completely unblended at the 1% level. Several molecular bands, notably the γ' system of TiO and the red system of CN, are prevalent in the 6100 Å region for a star with $T_{\rm eff} \sim 4250$ K. Weak neutral metal lines also are scattered throughout this interval (e.g., Kurucz and Hartmann 1984). Because of these blends, and the difficulty of treating them in Fourier space (Smith and Gray 1976), we have not attempted a Fourier analysis.

We have endeavored to remove "resolved" (i.e., obviously distinguishable) blends in two ways. If the main line to be studied is contaminated far in its wing (e.g., the blue wing 6173.3 Å in Fig. 2*d*), it was generally possible to remove the blend by a χ^2 fit to the composite line. If the blend is deeper in the shoulder of the line of interest, we usually found it easier to reflect part of the unblended wing across line center to replace the blended one. Points redward of 6154.41 Å in the 6154.2 Å profile (Fig. 2*a*), for example, were replaced with their blue wing counterparts. Our primary guide to confirm the reality of a given weak feature was the Sunspot Atlas of Harvey (1977). Affected portions of the blended line profiles were given less

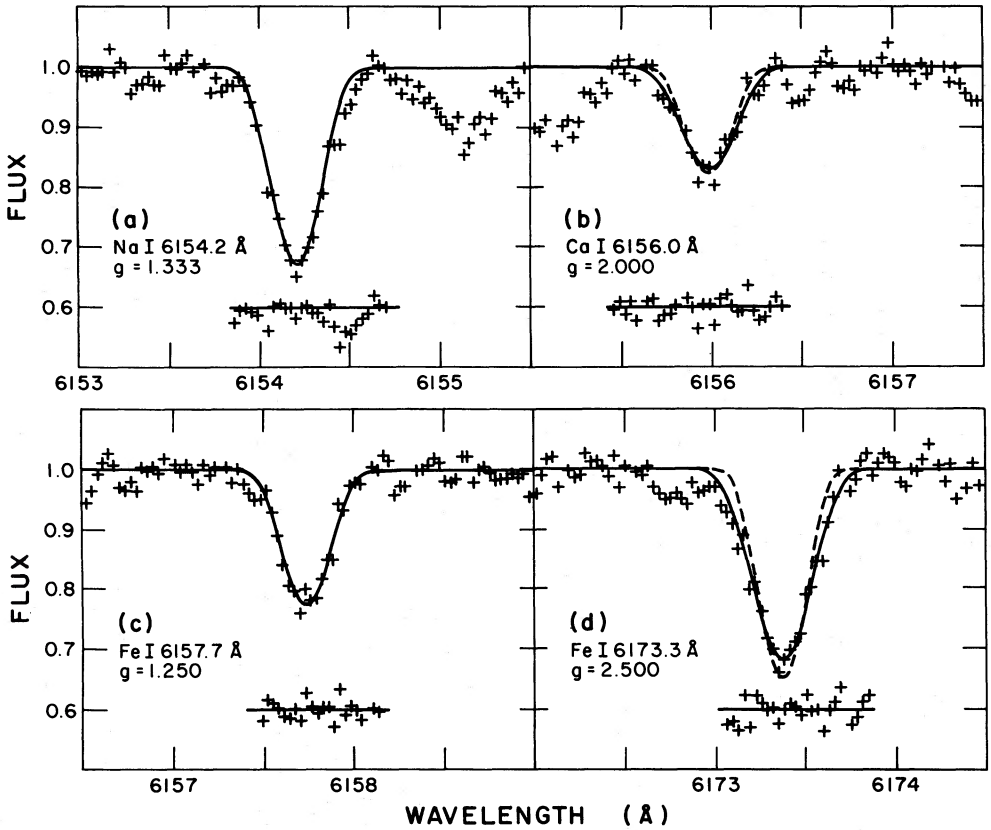

FIG. 2.—Examples of the magnetic flux profile modeling. Plus signs represent data (no blends removed), solid lines are the model fits, and dotted lines, shown with the high Landè *g* lines, are the models with no field, for comparison. All models have identical velocity broadening parameters. The scale is 0.03 Å per point, 2.5 points per resolution element. The residuals of the fits are shown below each modeled line, 0.6 being the zero level (*solid horizontal line*). The mean derived magnetic field parameters are $B = 2575$ G and $f = 0.78$.

weight in subsequent analyses. Profiles with blend depths greater than 5% of the continuum were not used.

Following the removal of weak blends, we next determined the velocity broadening parameters. Lines chosen for use in this stage of the analysis are listed in Table 3. Our criteria for selection were low magnetic sensitivity ($g \leq 1.333$), freedom from strong blends, and moderate strength (depths between 0.2 and 0.6 of the continuum). The local continuum was defined to be a line drawn through the average of the highest data points within ~ 1 Å to the blue and red of the line in question. We estimated a starting value for η_0 from the line depth and assumed $B = 0$; the remaining initial parameter values are given in Table 2. The macroturbulent velocity, ζ, was set at 3 km s^{-1}, since Vogt, Soderblom, and Penrod (1983) found that this value gave good fits to the line Ba II λ6141.7 of EQ Vir. Our derived rotational velocity, $v \sin i = 9.9 \pm 0.8$ km s^{-1}, agrees well with the Vogt *et al.* result of 10.8 km s^{-1} and is probably more reliable, owing to our higher resolution (75 versus 125 mÅ) and use of more lines (five instead of one). Low-g line models with magnetic fields (which are essentially velocity broadening fits, since the effect of B on the low-g profile is negligible) are shown in Figures 2*a* and 2*c*.

The derived values for the rotational and macroturbulent broadening were then used as fixed input in the Zeeman line-profile modeling. We employed the procedure outlined in § III*a*, first modeling a low-g line with a (η_0, ξ) fit (initially assuming $B = 0$), scaling its η_0 value, and then modeling the high-g line using these parameters as initial input to a three-parameter (η_0, B, f) fit. Successive iterations soon converged on the final f and B values. Starting values for the magnetic parameters are listed in Table 2. To make certain that the low-g comparison lines adequately represent the unsplit form of high-g lines (to within an opacity factor), we generally restricted the lines in our magnetic analysis to those pairs with similar ($\pm 30\%$) equivalent widths and lower level excitation potentials. This ensured that the line pairs have similar broadening parameters and should be formed at roughly the same temperature and level in the atmosphere. Since we account for the thermal component of the line profiles ($2kT_{\rm eff}/m_{\rm element}$) separately, it is safe to compare lines of different elements.

Figure 2 depicts representative model fits to four lines. Deviations of the fits from the data (plotted below the profiles) are typically at the noise level. The magnetic parameters derived for each line pair are compiled in Table 4. Despite the differences in atomic structure among the low-g lines used for comparison, the scatter in the derived f and B values is gratifyingly small. We assigned weights to each measurement according to the quality of the line profiles involved and their similarity in atomic structure, Landé g values, and excitation potential. A weighted average of the measurements yields $f = 0.78$ and $B = 2575$ G. The formal errors, computed by determining the parameter changes necessary to alter χ^2 of the fit by 1, are approximately ± 0.16 and ± 200 G for each line pair.

TABLE 4

SUMMARY OF MAGNETIC ANALYSIS OF EQ VIRGINIS LINES

Low-g Line	High-g Line	f	B	Analysis Type[a]	Assigned Weight
λ6151.6 Fe	λ6173.3 Fe	0.79	2700	W	0.9
λ6154.2 Na	λ6173.3 Fe	0.81	2600	W	0.7
λ6166.4 Ca	λ6173.3 Fe	0.80	2400	W	1.0
λ6180.2 Fe	λ6173.3 Fe	0.84	2600	W	1.0
λ6166.4 Ca	λ6151.6 Fe	0.74	2900	W	0.6
λ6180.2 Fe	λ6151.6 Fe	0.71	2600	W	0.5
λ6166.4 Ca	λ6156.0 Ca	0.75	2700	W	0.5
λ6173.3 Fe (61 Cyg A)	λ6173.3 Fe (EQ Vir)	0.79	2500	S	...

[a] W = wavelength domain analysis; S = interstar differential analysis.

We have also tested the sensitivity of the derived magnetic field parameters to errors in the other fitting parameters in order to obtain a better understanding of the overall uncertainties. To accomplish this, we arbitrarily changed particular fitting parameters one at a time and ran the analysis routine, noting changes in the derived field strength and filling factor. Since we normalize to unit strength before fitting, the results are relatively insensitive to η_0. Varying η_0 by a factor of 2 altered f and B by less than 3%. Lowering ξ by 1 km s^{-1}, on the other hand, increased the derived field strength by 6% and the filling factor by 14%. Raising ξ by 1 km s^{-1} increased f by 9% but lowered B by 11%. Altering $v \sin i$ by ± 1 km s^{-1} produced negligible changes in the magnetic parameters. Considering these additional uncertainties, together with the fact that the (f, B)-plane χ^2 minima were rather shallow and extended along lines of constant $B(f)^{1/2}$ (as noted also by Gray 1984*a*), we estimate our overall errors at ± 300 G and ± 0.14. The final results of the flux profile analysis are thus $B = 2575 \pm 300$ G and $f = 0.78 \pm 0.14$.

The profile modeling results are still subject to the effects of weak blends hidden within the analyzed profiles. To investigate the importance of "unresolved" blends to our derived magnetic parameters, we employed a variant of our modeling technique, one that we believe largely eliminates the effects of unseen blends. This second method relies on using a magnetic null star (where f and/or $B = 0$ by assumption) with the same spectral type and stellar parameters as the star of interest. We then compare high-g lines in the two stars directly. Once differences in rotational velocity have been accounted for, any differences between lines in the two stars will arise only from the Zeeman effect; that is, the "unresolved" blends should cancel out to first order when the two spectra are subtracted from each other. After subtracting the active star profile from that of the altered null star, we fit the resulting difference profile, $D(\lambda)$, with the model

$$D(\lambda) = \left[\frac{I_{\rm null\ star}}{I_c}(\lambda) - \frac{I_{\rm active\ star}}{I_c}(\lambda) \right] * V_{\rm active\ star}(\lambda) * M(\lambda) * i(\lambda) , \quad (7)$$

where we have implicitly assumed that the turbulence in the two stars is identical. These assumptions are reasonable, since ζ is a function primarily of $T_{\rm eff}$ (Gray 1984*b*) and ξ is fairly constant along the lower main sequence. This technique for removing blends also eliminates many problems involved in selecting and analyzing suitable low-g comparison lines, since the differenced lines have identical atomic parameters. Once the velocity broadening parameters have been determined for each star separately, the resulting χ^2 search in the most simple case thus involves only three parameters (η_0, f, B).

There are, however, a few drawbacks to the differential analysis technique. First, we must identify a null magnetic star. Typically, the best we can hope for is that the selected star has B and/or f values so low that the apparent Zeeman broadening of the profiles is negligible. For the present study we thus

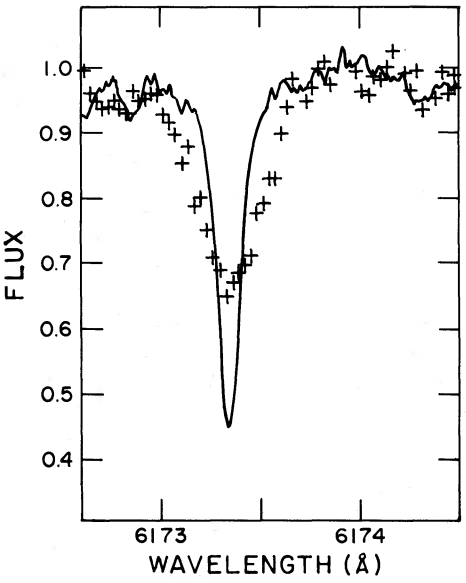

FIG. 3*a*

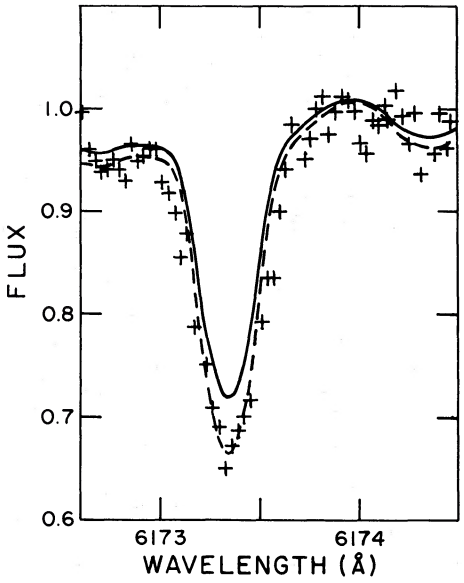

FIG. 3*b*

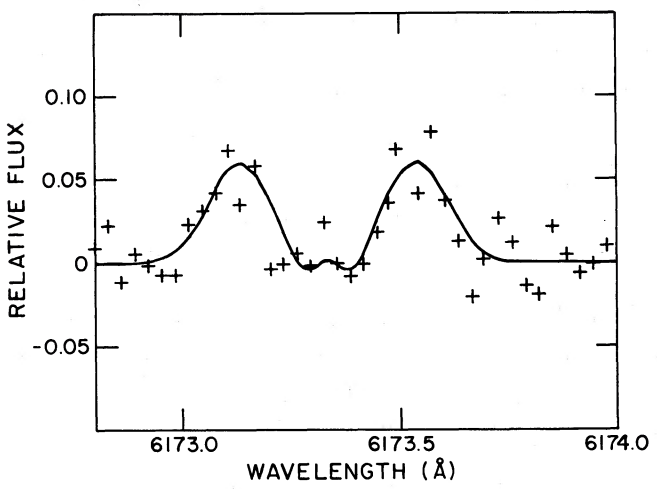

FIG. 3*c*

FIG. 3.—(*a*) Differential magnetic analysis; unmodified profiles of EQ Vir and Marcy's 61 Cyg A in the region of 6173 Å. Solid line depicts the spectrum of 61 Cyg A; plus signs are data from EQ Vir. (*b*) Same as (*a*), but the 61 Cyg A spectrum (*solid line*) has been artificially spun up to equal the $v \sin i$ of EQ Vir. Dashed line shows the same 61 Cyg profile altered to account for the abundance difference between the two stars. Excess broadening due to the Zeeman effect is evident. (*c*) Resulting fit (*solid line*) to difference spectrum in the wavelength domain. The derived field parameters are $B = 2500$ G and $f = 0.79$.

searched for stars of the same spectral type as EQ Vir but with very weak signatures of magnetic activity, i.e., low Ca H and K and X-ray fluxes, weak UV emission, and long rotation periods. A second problem is that there is no guarantee that two stars of the same spectral type and effective temperature will have identical atmospheres. It is possible that differences in other parameters, such as turbulence, abundance, surface gravity, or temperature structure changes resulting from the magnetic fields themselves, could alter the line profiles of the active star relative to those of the null star. In undertaking our analysis, we presume that these are all second-order effects compared with the Zeeman broadening itself.

Results of the differential Zeeman analysis are illustrated in Figures 3*a*–3*c*. Figure 3*a* compares a small portion of our EQ Vir spectrum around the 6173.3 Å ($g = 2.5$) line with a section of a 61 Cyg A spectrum, our selected magnetic null star. The 61 Cyg A data were kindly supplied by Dr. Geoff Marcy and have similar spectral resolution (65 versus 75 mÅ) to our own. The star 61 Cyg A is an old, inactive, K5 dwarf with a rotational period of 37.9 days (Vaughan *et al.* 1981), low average Ca II emission (Noyes *et al.* 1984), weak UV emission, low X-ray luminosity ($\log L_x = 27.5$; Vaiana *et al.* 1981), and a $B-V$ color of 1.18 (identical with that of EQ Vir), thereby satisfying our criteria for a magnetic null star. We adopt $v \sin i = 1$ km s^{-1} for 61 Cyg A, based on its rotational period and an assumed radius of 0.7 $R_\odot$. Figure 3*b* compares the two stars after the 61 Cyg A spectrum has been artificially "spun up" to EQ Vir's rotational rate and degraded slightly to the resolution of the MMT observations (*solid curve*). Lines in the EQ Vir spectrum are visibly broader, but this effect is masked somewhat by the smaller equivalent widths of the 61 Cyg A lines, which are due to a magnetically induced increase in equivalent width in EQ Vir (e.g., Stepanov 1958) and a small abundance difference between the two stars. To make a better visual comparison of the profiles, we logarithmically scale (Marcy 1984) the altered 61 Cyg A spectrum to mimic an increase in abundance (Fig. 3*b*, *dotted line*) and observe that excess broadening in the EQ Vir line is still discernible. We consider this to be further evidence that a large field covers much of the surface of EQ Vir. Taking the abundance difference into account, careful examination of the (B, f)-plane of the χ^2 hypersurface reveals that the deepest minimum lies at $B = 2200 \pm 300$ G and $f = 0.57 \pm 0.22$, somewhat different from our previous results.

Unresolved blends and/or a nonzero field on 61 Cyg A are likely reasons for this discrepancy. Marcy (1984) has analyzed the identical 61 Cyg A spectrum and found $B = 2660$ G and $f = 0.30$ by comparing 6173 Å with the $g = 1.00$ Fe I 6240 Å line. (Note that this filling factor is sufficiently small that 61 Cyg A is still a useful *relative* magnetic null for EQ Vir with $f \sim 0.78$.) If unresolved blends affect the 61 Cyg A spectra, Marcy's field and filling factor may well be too large and our differential model results will be roughly correct, blends having

altered profile modeling results. If, on the other hand, unresolved blends are not important, the nonzero f and B of 61 Cyg A will have altered the derived field for EQ Vir in a differential analysis. To test the change this might produce, we reanalyzed the EQ Vir data differentially, this time assuming Marcy's field parameters for 61 Cyg A. The analysis yielded $B = 2500 \pm 300$ G and $f = 0.79 \pm 0.22$ (Fig. 3*c*), in good agreement with the profile modeling results, but not inconsistent (within the large errors) with the original differential analysis. Although the actual amount of blending or fields in the 61 Cyg A spectrum is thus still unclear, we take the agreement with the profile modeling to indicate that this second differential analysis is more nearly correct. We plan a more detailed analysis in the future, using many line pairs, once we have obtained a high S/N, broad-band spectrum of 61 Cyg A. Such a study should clear up the question of unresolved blends and their effect on the 61 Cyg A and EQ Vir spectra.

The value we derive for the surface-area coverage is model dependent (see § IV). Deviations from our assumptions concerning the spatial structure (through $\langle\gamma\rangle$) and the actual continuum brightness and line strengths in the magnetic regions will affect the resulting value of f. Within our assumptions, however, and combining the results of our two rather different analysis methods, we conclude that the active regions on EQ Vir cover $\sim 80\% \pm 15\%$ of its surface and contain an average magnetic field strength of $\sim 2500 \pm 300$ G.

IV. DISCUSSION

The question now arises as to the type of magnetic region we have detected on EQ Vir. To explore the possible contribution from starspots, we relax our assumption that the continuum fluxes in the magnetic and nonmagnetic regions are equal, and construct a model with $f_Q + f_S = 1$ and the total stellar flux given by

$$F_Q f_Q + F_S f_S = F_{\rm total} , \tag{8}$$

where F_Q, F_S, f_Q, and f_S stand for the fluxes and filling factors in the quiet and spotted regions, respectively. These quantities are related to our model through the relations $f = F_S f_S / F_{\rm total}$ and $1 - f = F_Q f_Q / F_{\rm total}$, and thus $F_S f_S = 0.8 F_{\rm total}$ and $F_Q f_Q = 0.2 F_{\rm total}$. We now compare EQ Vir's photometric amplitude of $\Delta m_V = 0.1$ (Bopp and Fekel 1977) with the magnetic analysis results. If we take the limiting case of one stellar hemisphere being completely free of spots, we have $F_Q = F^U_{\rm total}$ on the unspotted hemisphere, and $F_Q f_Q + F_S f_S = 0.9 F^U_{\rm total}$ on the dimmer, spotted hemisphere. Solving the five equations simultaneously yields $f_Q = 0.18$, $f_S = 0.82$, and $F_S/F_Q = 0.88$. This inferred spot filling factor is very large and raises questions about the stability of the spots against coalescence and annihilation of magnetic flux. Worse still, if we take Vogt's (1982) value of $T_{\rm spot}/T_{\rm eff} \approx 0.85$ for the dM0e flare star BY Dra and apply it to EQ Vir, we compute an expected ratio of continuum fluxes $B_v(T_{\rm spot})/B_v(T_{\rm eff}) = 0.4$ at 6100 Å, clearly inconsistent with $F_S/F_Q = 0.88$. We therefore conclude that the fields we have measured arise primarily from bright active regions—perhaps the stellar analogs of solar network and plage.

Continuing in this line of thought, we can construct a similar model of EQ Vir dominated by bright magnetic regions. In the limiting case we have a dimmer "network"-free hemisphere with $F_Q = 0.9 F^A_{\rm total}$ and an active hemisphere with $F_Q f_Q + F_N f_N = F^A_{\rm total}$, where F_N and f_N are the network flux and filling factor, respectively. Solving this system yields $f_Q = 0.22$, $f_N = 0.78$, and $F_N/F_Q = 1.14$, a reasonable value. In reality, EQ Vir certainly has some admixture of spots on its surface as well; these will reduce f_N and perhaps raise the inferred F_N/F_Q, since now $F_N f_N + F_S f_S = 0.8 F_{\rm total}$ and $f_N + f_S + f_Q = 1$. Thus 80% is likely an overestimate of the surface-area coverage of magnetic regions. It is probably not very wrong, however, since F_N/F_Q is not very much greater than unity, so for simplicity, and to facilitate comparison with previous results, we retain $f = 0.80$, with the caveat that it is strictly accurate only if $F_N = F_Q$.

The results of our study have several important implications. First, predicted values of surface fields on flare stars in the literature appear to be too large. EQ Vir has a field strength of 2500 G, and although it is among the warmest of the flare stars, it seems unlikely that cooler dMe stars have substantially stronger fields. Our results therefore run counter to estimates by Mullan (1975) of network/plage fields on these stars in the range of 5–10 kG based on scaling arguments from his starspot models. We cannot say whether Mullan's (1974) spot models overestimate field strengths as well (he calculates values of 10–20 kG), however, owing to the low continuum flux ratio F_S/F_Q. A careful search of the continuum around the high-g 6173.3 Å line for symmetrically placed, widely split σ components that might be due to 10–20 kG fields shows no likely features down to the limit of our photometric accuracy of $\sim 2\%$, corresponding to an apparent filling factor of $f \lesssim 0.04$. The true spot filling factor, however, will be this value corrected for the contrast ratio between spot and photosphere, $f^{\rm true}_{\rm spot} = f^{\rm apparent}_{\rm spot}/(F_S/F_Q)$. Using $F_S/F_Q = 0.4$, we find that $f^{\rm true}_{\rm spot} \lesssim 0.10$. Conceivably, then, up to $\sim 10\%$ of the surface of EQ Vir could have been covered by 10–20 kG fields in spots at the time of our observations and escaped our detection. Thus Mullan's predicted spot field strengths are still possible, but we reiterate that his plage/network estimates are probably too high.

Vogt (1980) has observed EQ Vir in circularly polarized light and found no fields above his detection threshold of $B \approx 100$ G. Our positive detection of $B = 2500$ G indicates that a complex field geometry effectively cancels the largest part of the polarization signal from EQ Vir (cf. Borra, Edwards, and Mayor 1984). Like the Sun, EQ Vir probably has many regions with oppositely directed field lines. More speculatively, we can estimate the minimum number of active areas EQ Vir must possess in order to reduce its polarization signature to below the observed limit by comparing our field strength and area coverage with Vogt's upper limits. Following Borra, Edwards, and Mayor (1984), we assume that the bright magnetic areas on a star are of equal intensity, size, and field strength and are uniformly distributed over the stellar surface. The minimum number of dipole magnetic areas is then approximately

$$N \gtrsim (Bfq/B_{\rm pol})^2 , \tag{9}$$

where $B_{\rm pol}$ is upper limit to the net magnetic field derived from polarization studies and q is the fractional longitudinal field in a typical magnetic area. Unfortunately, the value of q integrated over the stellar surface is highly dependent on the actual magnetic geometry. If, however, we assume that the fields are roughly radial everywhere (Marcy 1982), we have $q \approx \langle B \cos\gamma\rangle/\langle B\rangle = \langle\cos\gamma\rangle = 2/\pi$. Taking $B_{\rm pol} = 100$, we then find $N \gtrsim 160$.

A second implication of our results is that the 2500 G field is consistent with equipartition of magnetic and thermal energy densities in the photosphere. If we compare the photospheric pressure at $\tau_{5000} = 1$ from a standard solar model ($P = 1.173 \times 10^5$ dynes cm^{-2}; Vernazza, Avrett, and Loeser

1981), and at $\tau_{\text{Rosseland}} = 1$ from a 4250 K M dwarf model ($P = 3.895 \times 10^5$ dynes cm^{-2}; Mould 1976), we find $P(\text{dM})/P(\text{Sun}) = 3.32$. Energy equipartition implies $B^2/8\pi \sim P$, or $B_{\text{EQ Vir}} \approx [P(\text{dM})/P(\text{Sun})]^{1/2} B_\odot$. Taking a typical solar plage field to be 1500 G (Tarbell and Title 1977), we calculate $B_{\text{EQ Vir}} \approx 2730$ G, in good agreement with our derived value. The gas-pressure confinement of flux tubes suggested by this accord has also been proposed to explain the strength of solar network fields (e.g., Parker 1981) and the lack of detection of fields in active giants (equipartition implies fields below observable limits; Marcy and Bruning 1984).

The magnetic parameters of EQ Vir may also be considered in another way. Defining a surface-averaged field as $\langle B \rangle \equiv fB$, EQ Vir's averaged field is about 2000 G. We can compare this value with previous measurements. If all magnetic field measurements on dwarfs derived using unpolarized line profiles are placed on a common filling-factor scale (i.e., making $\langle \gamma \rangle = 34°$) and three measurements are excluded (those of the Sun, EQ Vir, and RWH's detection of 70 Oph at poor S/N), we find that $\langle B \rangle_{\text{average}} \approx 630 \pm 130$ (1 σ) G. Thus EQ Vir stands out as having more than 3 times the average magnetic field of the typical active chromosphere G and K dwarfs studied to date. In fact, $\langle B \rangle_{\text{EQ Vir}}$ is nearly a factor of 2 larger than the largest $\langle B \rangle$ previously measured (ξ Boo A, with $\langle B \rangle \sim 1100$ G; RWH) and a factor of ~ 130 greater than that of the Sun (with $\langle B \rangle \sim 15$ G). (We note, however, that it may be dangerous to compare our results with those of previous studies that neglect radiative transfer and line-blending effects.)

One possible reason for EQ Vir's unusually large magnetic field production is its short rotational period of ~ 4 days and hence high angular velocity (Ω). Most dynamo theories predict that the generation of stellar magnetic fields should be proportional to some power of Ω (e.g., Durney and Robinson 1982). The relative constancy of $\langle B \rangle$ at lower levels for other active dwarf stars, however, argues that a rather substantial drop in magnetic field generation occurs for periods longer than some critical value greater than 4 days. Corollary evidence for this is seen in the X-ray data, where Walter (1982) finds a "break" in the X-ray activity-rotation relations at $P \sim 10$ days. Perhaps at $P \sim 10$ days the magnetic field generation changes its dependence on Ω, possibly due to a change in the mode of the dynamo (Durney and Robinson 1982) or its convective pattern (Knobloch, Rosner, and Weiss 1981). On the other hand, a *sudden* change in the dynamo mechanism seems ruled out by smooth dependences seen between stellar parameters and activity indicators such as Ca II emission, X-ray fluxes, and transition region lines (see, for example, Noyes *et al.* 1984; Mangeney and Praderie 1984; Vilhu 1984).

Further measurements of magnetic fields for stars with periods in the 3–10 day range should help clarify the dependence of $\langle B \rangle$ on rotation, thereby furthering our understanding of dynamos and magnetic flux generation.

We extend our thanks to Drs. Geoff Marcy and Tom Ayres for many valuable discussions, and to Drs. David Bruning and Steven Vogt, the referee, for helpful suggestions. We also thank Dr. David Latham and the MMT staff for providing assistance in the observational program. We gratefully acknowledge support from the National Aeronautics and Space Administration through grant NGL-06-003-057 to the University of Colorado.

REFERENCES

Anderson, C. M. 1979, *Pub. A.S.P.*, **91**, 202.
Anderson, C. M., Hartmann, K. W., and Bopp, B. W. 1976, *Ap. J. (Letters)*, **204**, L51.
Auer, L. H., Heasley, J. N., and House, L. L. 1977, *Solar Phys.*, **55**, 74.
Bopp, B. W. 1974, *M.N.R.A.S.*, **46**, 108.
Bopp, B. W., and Fekel, F. 1977, *A.J.*, **82**, 490.
Borra, E. F., Edwards, G., and Mayor, M. 1984, *Ap. J.*, **284**, 211.
Brown, D. N., and Landstreet, J. D. 1981, *Ap. J.*, **246**, 899.
Cram, L. E., and Mullan, D. J. 1979, *Ap. J.*, **234**, 579.
Cram, L. E., and Woods, D. T. 1982, *Ap. J.*, **257**, 269.
Durney, B. R., and Robinson, R. D. 1982, *Ap. J.*, **253**, 290.
Giampapa, M. S., Golub, L., and Worden, S. P. 1983, *Ap. J. (Letters)*, **268**, L121.
Gray, D. F. 1976, *The Observation and Analysis of Stellar Photospheres* (New York: Wiley).
———. 1984*a*, *Ap. J.*, **277**, 640.
———. 1984*b*, *Ap. J.*, **281**, 719.
Harvey, J. W. 1977, *A Photographic Spectral Atlas of a Sunspot between 3813 and 9182 Å* (Tucson: Kitt Peak National Observatory).
Knobloch, E., Rosner, R., and Weiss, N. O. 1981, *M.N.R.A.S.*, **197**, 45P.
Kunkel, W. E. 1975, in *IAU Symposium 67, Variable Stars and Stellar Evolution*, ed. V. E. Sherwood and L. Plaut (Dordrecht: Reidel), p. 15.
Kurucz, R. L., and Hartmann, L. 1984, Smithsonian Astrophysical Observatory preprint, No. 2015.
Latham, D. W. 1982, in *IAU Colloquium 67, Instrumentation for Astronomy with Large Optical Telescopes*, ed. C. M. Humphries (Dordrecht: Reidel), p. 259.
Linsky, J. L. 1980, *Ann. Rev. Astr. Ap.*, **18**, 115.
———. 1983, in *IAU Symposium 102, Solar and Stellar Magnetic Fields: Origins and Coronal Effects*, ed. J. O. Stenflo (Dordrecht: Reidel), p. 313.
Linsky, J. L., Bornmann, P. L., Carpenter, K. G., Wing, R. F., Giampapa, M. S., Worden, S. P., and Hege, E. K. 1982, *Ap. J.*, **260**, 670.
Mangeney, A., and Praderie, F. 1984, *Astr. Ap.*, **130**, 143.
Marcy, G. W. 1982, *Pub. A.S.P.*, **94**, 562.
———. 1984, *Ap. J.*, **276**, 286.
Marcy, G. W., and Bruning, D. H. 1984, *Ap. J.*, **281**, 286.
Moore, C. E., Minnaert, M. G. J., and Houtgast, J. 1966, *The Solar Spectrum, 2935 Å to 8770 Å*, NBS Monog., No. 61.
Mould, J. R. 1976, *Astr. Ap.*, **48**, 443.
Mullan, D. J. 1974, *Ap. J.*, **192**, 149.
———. 1975, *Astr. Ap.*, **40**, 41.
Noyes, R. Q., Hartmann, L. W., Baliunas, S. L., Duncan, D. K., and Vaughan, A. H. 1984, *Ap. J.*, **279**, 763.
Parker, E. N. 1981, in *Solar Phenomena in Stars and Stellar Systems*, ed. R. M. Bonnet and S. K. Dupree (Dordrecht: Reidel), p. 33.
Robinson, R. D. 1980, *Ap. J.*, **239**, 961.
Robinson, R. D., Worden, S. P., and Harvey, J. W. 1980, *Ap. J. (Letters)*, **236**, L155 (RWH).
Saar, S. H. 1986, in preparation.
Smith, M. A., and Gray, D. F. 1976, *Pub. A.S.P.*, **88**, 809.
Stepanov, V. E. 1958, *Izv. Krymsk. Ap. Obs.*, **18**, 136.
Tarbell, T. D., and Title, A. M. 1977, *Solar Phys.*, **52**, 31.
Vaiana, G. S., *et al.* 1981, *Ap. J.*, **245**, 163.
Vaiana, G. S., and Rosner, R. 1978, *Astr. Ap.*, **16**, 393.
Vaughan, A. H., Jr., Baliunas, S. L., Middelkoop, F., Hartmann, L. W., Mihalas, D., Noyes, R. W., and Preston, G. W. 1981, *Ap. J.*, **250**, 276.
Vernazza, J. E., Avrett, E. H., and Loeser, R. 1981, *Ap. J. Suppl.*, **45**, 635.
Vilhu, O. 1984, *Astr. Ap.*, **133**, 117.
Vogt, S. S. 1980, *Ap. J.*, **240**, 567.
———. 1982, in *IAU Colloquium 71, Activity in Red Dwarfs*, ed. P. B. Byrne and M. Rodonò (Dordrecht: Reidel), p. 137.
Vogt, S. S., Soderblom, D. R., and Penrod, G. D. 1983, *Ap. J.*, **269**, 250.
Walter, F. H. 1982, *Ap. J.*, **253**, 745.
Zwaan, C. 1981, in *Solar Phenomena in Stars and Stellar Systems*, ed. R. M. Bonnet and A. K. Dupree (Dordrecht: Reidel), p. 463.

JACQUES M. BECKERS: Advanced Development Program, National Optical Astronomy Observatories, P.O. Box 26732, Tucson, AZ 85726

JEFFREY L. LINSKY and STEVEN H. SAAR: Joint Institute for Laboratory Astrophysics, University of Colorado, Boulder, CO 80309 0440